Nonisothermal cold crystallization of poly(ethylene terephthalate)

Renate M.R. Wellen[a)]
Department of Chemical Engineering, Federal University of Pernambuco, Recife, Pernambuco 50670-901, Brazil
Eduardo Canedo and Marcelo S. Rabello
Department of Materials Engineering, Federal University of Campina Grande, Campina Grande, Paraíba 58249-140, Brazil

(Received 13 September 2010; accepted 12 January 2011)

The thermal transitions and the nonisothermal cold crystallization kinetics of poly(ethylene terephthalate) (PET) at constant heating rates were investigated using differential scanning calorimetry. It was found that the glass transition and crystallization temperature increased with the heating rates, while the melting temperature showed a little variation for the heating rates used. Crystallization and melting latent heats were remarkably constant, independent of the heating rate. Kinetics parameters were determined using Ozawa model. Two different kinetic regimes were identified, corresponding to primary and secondary crystallization, at low and high fractional crystallization, respectively, both following Ozawa's model. Kinetics parameters were determined for the primary and secondary regimes; the pre-exponential constant (K_T) and Ozawa's exponent (m) decreased with increasing crystallization temperature. The combined kinetic parameter $Z=K_T^{1/m}$ increased exponentially with temperature; activation energies were estimated using Arrhenius plots for the two PET crystallization regimes.

I. INTRODUCTION

Poly(ethylene terephthalate) (PET) is a thermoplastic resin used in several industrial segments, including film, fiber, injected, and blown products. PET can be obtained in amorphous or semicrystalline states; in the later case, its properties depend strongly on the degree of crystallinity.

Engineering grades of PET for injection molding applications are highly crystalline and require fast crystallization at relatively low temperature to maintain high impact strength. However, film and bottle grades, used for transparent products, require amorphous or low crystalline morphology, stable at processing conditions. Thus, crystallinity and crystallization rates are very important considerations when selecting a resin grade and developing a process.

Structural unit of PET includes aliphatic and aromatic groups in the main chain. Aliphatic segments are flexible but the rigid aromatic groups increase the stiffness of the chain, hindering the crystallization process. A semicrystalline polymer like PET can develop a crystalline structure when cooled from the melt or heated from the glassy state, either under isothermal or under nonisothermal conditions. Two competing factors affect the crystallization behavior: cooling/heating rate and crystal nucleation and growth rates. The resulting microstructure has a significant effect on the ultimate properties of the product, such as elasticity, permeability, transparency, and stiffness.[1,2]

Although more difficult to study than crystallization under isothermal conditions, the quantitative evaluation of nonisothermal crystallization is required to understand and model industrial processes, which are conducted under nonisothermal conditions.[3–9]

Several studies of nonisothermal crystallization of PET are available in the literature. Jabarin[10] reported the crystallization behavior of PET under nonisothermal conditions as a function of molar mass, polycondensation catalyst system, and polymerization conditions. He showed that it is possible to establish the minimum cooling rate required to produce PET without detectable crystallinity. Cooling requirements to produce noncrystalline PET depend on molecular mass and, more importantly, on the catalyst system used in the polycondensation. The absence of crystallinity is a necessary requirement to produce optically clear products. In a similar study, Fann et al.[11] showed that different cooling modes can be used to optimize the conditions needed to keep crystallinity to a minimum during the production of PET bottles. The kinetic parameters for PET crystallization indicated that the competing process of nucleation and growth of PET spherulites during the cooling process were the controlling factors that determined the degree of crystallinity in the final PET products. Lu and Hay[12] analyzed the effect of physical aging on cold crystallization rate of PET; they observed an increase of the cold crystallization rate with

[a)]Address all correspondence to this author.
e-mail: wellen.renate@gmail.com
DOI: 10.1557/jmr.2011.44

 © Materials Research Society 2011

https://doi.org/10.1557/jmr.2011.44 Published online by Cambridge University Press

physical aging, attributed to an increase in the nucleation density. Sajkiewicz et al.[13] studied nonisothermal crystallization of PET from the melt under dynamic conditions and used Ozawa model to analyze the crystallization kinetics.

However, few studies dealt with the nonisothermal cold crystallization kinetics of PET, a process of great practical and scientific importance. Nonisothermal cold crystallization studies can be useful to understand the relationship between processing, structure, and properties. The present work is concerned with the cold crystallization kinetics of PET under nonisothermal conditions. This follows a previous study involving the isothermal cold crystallization of PET.[14]

II. EXPERIMENTAL

A. Materials

The film-grade PET used in this work was supplied by Terphane (Brazil) as extruded "amorphous" clear film of 0.5-mm thickness, with intrinsic viscosity of 0.7 dL/g measured in *o*-chlorophenol.

B. Methods

Differential scanning calorimetry (DSC) is a versatile tool for thermal analysis of materials. A small sample of the material is heated or cooled at a programmed temperature variation rate, and the rate of energy absorbed (endothermic process) or liberated (exothermic process) by the material is monitored, along with the temperature, as a function of time. In this way, specific heats, latent heats of phase change, and many other physical or chemical reactions can be quantitatively identified. DSC is particularly suited for the thermal analysis of polymeric materials.[15,16]

DSC measurements were carried on a Shimadzu DSC-50 (Kyoto, Japan). The nonisothermal cold crystallization was studied by heating the samples from ambient temperature to 300 °C, at rates ranging from 2.5 to 40 °C/min. To avoid uneven thermal conduction through the samples, which may cause differential broadening and shifting of the peaks,[17] the same amount of polymer (8 ± 1 mg) was used in all tests. From the DSC thermograms, the thermal properties and the kinetic parameters were obtained, and this will be described throughout the text.

III. RESULTS AND DISCUSSION

The DSC provides graphical/numerical output in the form of the rate of heat transfer (power) J to the sample as a function of either time (t) or sample temperature (T). When a polymer like PET is analyzed as a function of temperature, the first main thermal effect is the glass transition (Fig. 1), corresponding to a change from the glassy to the rubbery phase. As the temperature increases, the amorphous phase gains mobility and a cold crystallization phenomenon takes place, yielding an exotherm peak. Finally, an endotherm melting peak is observed.

A. Transition temperatures and crystallinity

Glass transition temperature (T_g), crystallization temperature (T_c), and melting temperature (T_m) were estimated for all heating rates (q) from the DSC output according to ASTM D-3418. The results are shown in Table I and Fig. 2.

The glass transition and cold crystallization temperatures increased with increasing heating rates: 14 and 23 °C, respectively, when heating rate changes from 2.5 to 40 °C/min. On the other hand, the melting temperature is only slightly affected by the heating rate: $T_m = 255 \pm 1$ °C over the same interval of heating rates.

Glass transition is a phenomenon of molecular relaxation. At a faster heating rate less time is available for relaxation, shifting the transition to higher temperatures. Similar behavior was observed in PET/SAN[18] blends during cold crystallization with similar heating rates.

The increase in crystallization temperature with increasing heating rates suggests that, at higher rates, the motion and rearrangement of PET molecules are not fast enough to form the necessary nuclei for crystallization,

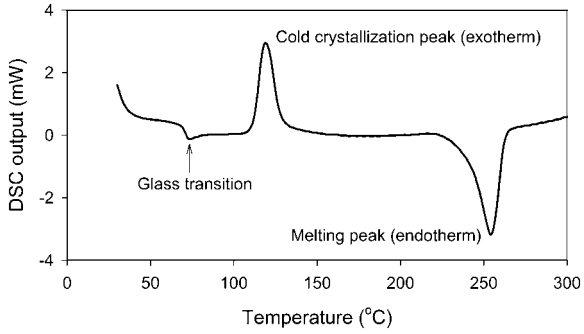


FIG. 1. Typical differential scanning calorimetry (DSC) plot for "amorphous" poly(ethylene terephthalate) (PET) sample heated a constant rate of 10 °C/min.

TABLE I. Transition temperatures of poly(ethylene terephthalate) (PET) at several heating rates.

q (°C/min)	T_g (°C)	T_c (°C)	T_m (°C)
2.5	65.3	109.3	256.8
5	66.4	112.1	255.2
7.5	67.5	113.4	254.4
10	70.9	120.1	254.9
15	71.9	123.1	253.9
20	73.8	126.0	253.9
30	77.0	129.1	257.5
40	79.3	132.2	256.0

https://doi.org/10.1557/jmr.2011.44 Published online by Cambridge University Press

compared to the lower temperatures attained at lower heating rates, where the specimen remains at each temperature for a longer time.[19,20] The opposite trend is observed for nonisothermal melt crystallization.[21,22]

The negligible variation of melting temperature with heating rate may be associated with the stability of the crystals, suggesting that the size and/or perfection of the crystals are the same for all conditions used. Comparable behavior was observed by Yoshihara et al.[23] and Jang et al.[24] for PET and PET/PS-*co*-MA (copolymer of styrene and maleic anhydride), respectively.

Latent heats (enthalpies) of crystallization (ΔH_c) and melting (ΔH_m) per unit mass were determined from the area under the peaks of the DSC output according to Eq. (1):

$$\Delta H_{trans} = \frac{\int_{T_1}^{T_2} |J(T)|\, dT}{m_S} \quad , \qquad (1)$$

where $J(T)$ is the DSC output in terms of temperature, T_1 and T_2 are the onset and end temperatures of the corresponding peak, and m_S is the mass of the sample. The results are shown in Fig. 3 (see also Table II).

Both latent heats show a moderate decrease with an increase in the heating rate, but the difference between the latent heat of melting and crystallization is remarkably constant, independent of the heating rate.

We assume that, above the glass transition temperature, a rubbery amorphous phase that includes a small, but not negligible, amount of crystalline polymer (initial crystallinity X_0) undergoes a process of cold crystallization at the crystallization temperature T_c, whereas the crystallinity of the sample reaches the "ultimate" crystallinity of the solid material (X_∞). Then, as the temperature increases, the crystalline phase melts at the melting temperature T_m, resulting in fully molten polymer (zero crystallinity).

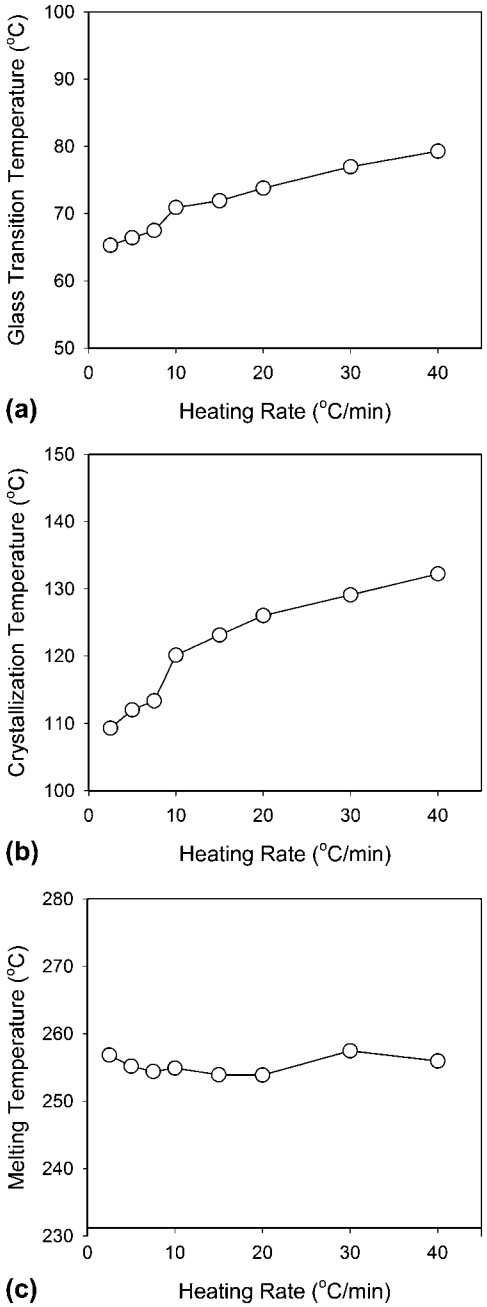


FIG. 2. Measured transition temperatures as functions of the heating rate: (a) glass transition, (b) cold crystallization, and (c) melting.

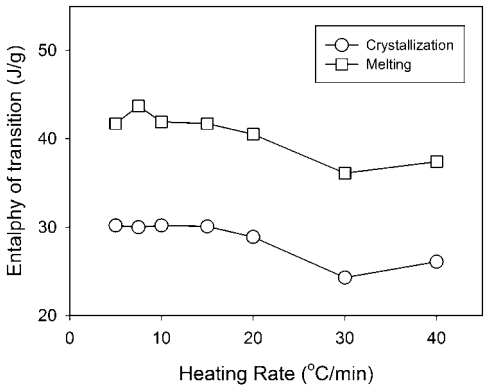


FIG. 3. Enthalpies of transition of PET as functions of the heating rate.

TABLE II. Latent heats of crystallization and melting and crystallinity of PET at several heating rates.

q (°C/min)	ΔH_c (J/g)	ΔH_m (J/g)	X_∞ (%)	X_0 (%)
2.5	26.4	29.4	21.0	–
5	30.2	41.7	29.8	3.7
7.5	30.0	43.7	31.2	5.4
10	30.2	41.9	29.9	4.1
15	30.1	41.7	29.8	4.2
20	28.9	40.5	28.9	4.5
30	24.3	36.1	25.8	5.2
40	26.1	37.4	26.7	4.8

https://doi.org/10.1557/jmr.2011.44 Published online by Cambridge University Press

From the experimentally determined heat of melting at each heating rate and the heat of melting of pure crystalline PET at the melting point, taken from the literature,[25] $\Delta H_m^0(T_m) = 140$ J/g, the ultimate crystallinity (X_∞) was computed for each heating rate:

$$X_\infty = \frac{\Delta H_m}{\Delta H_m^0(T_m)} \quad . \tag{2}$$

The ultimate crystallinity is fairly independent of the heating rate: $X_\infty \approx 29 \pm 2\%$ (Table II and Fig. 4).

The initial crystallinity of the samples (X_0) may be estimated from the equivalent of Eq. (2) for the cold crystallization process:

$$X_\infty - X_0 = \frac{\Delta H_c}{\Delta H_m^0(T_c)} \quad , \tag{3}$$

where $\Delta H_m^0(T_c)$ is the heat of melting of pure crystalline PET at the cold crystallization temperature, which is related to a reference value (at the crystalline melting point) through[26]

$$\Delta H_m^0(T_c) = \Delta H_m^0(T_m) - \Delta C_p(T_m - T_c) \quad , \tag{4}$$

where $\Delta C_p = C_p^{(a)} - C_p^{(c)}$ is the difference between the specific heat of the amorphous ($C_p^{(a)}$) and crystalline ($C_p^{(c)}$) phases; Eq. (4) assumes that the specific heat difference is independent of the temperature in the range between cold crystallization and melting (roughly, 120–255 °C), which is a reasonable approximation.

Specific heats of PET can be estimated using standard techniques and literature values. Assuming a linear relationship for the temperature dependence of the specific heat, we have

$$\begin{aligned} C_p^{(a)}(T) &= C_p^{(a)}(T_{ref})\left[1 + \beta^{(a)}(T - T_{ref})\right] \\ C_p^{(c)}(T) &= C_p^{(c)}(T_{ref})\left[1 + \beta^{(c)}(T - T_{ref})\right] \end{aligned} \quad , \tag{5}$$

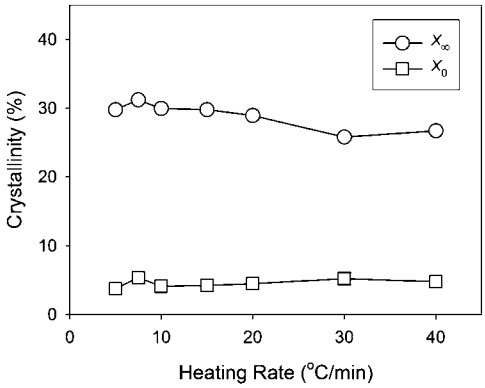


FIG. 4. Ultimate (X_∞) and initial (X_0) crystallinities of PET as functions of the heating rate.

where $\beta^{(a)}$ and $\beta^{(c)}$ are temperature coefficients for the amorphous and crystalline phases, respectively, and T_{ref} is a reference temperature. Using accepted literature values for $T_{ref} = 25$ °C,[27] we obtain $C_p^{(a)} \approx 1.85$ J/g °C and $C_p^{(c)} \approx 1.68$ J/g °C, computed at the average temperature between cold crystallization ($T_c = 120 \pm 10$ °C) and melting ($T_m = 256$ °C), i.e., $T \approx 188$ °C. Thus, $\Delta C_p \approx 0.17$ J/g K.

On the basis of Eqs. (3) and (4), the initial crystallinity may be estimated as $X_0 \approx 4.6 \pm 0.6\%$ (Table II and Fig. 4).

B. Crystallization rates

The fractional crystallization (or relative crystallinity) during a cold crystallization process may be defined as

$$x = \frac{X - X_0}{X_\infty} \quad , \tag{6}$$

where X is the crystallinity developed at time t (or temperature T), estimated by integration of the DSC peak from the onset of the crystallization:

$$x(T) = \frac{\int_{T_1}^{T} |J(T)|\, dT}{\int_{T_1}^{T_2} |J(T)|\, dT} \quad , \tag{7}$$

where $J(T)$ is the DSC output in terms of temperature, T_1 and T_2 are the onset and end temperatures of the cold crystallization peak, and T is an intermediate temperature, $T_1 \le T \le T_2$. The fractional crystallization may be considered as a function of either time (t) or temperature (T) because the temperature is a linear function of time at constant heat rate:

$$T = T_0 + qt \quad , \tag{8}$$

where $q = dT/dt$ is the heating rate and T_0 is the temperature at the starting point of the experiment.

Figure 5 shows the fractional crystallization as a function of both time and temperature for selected heating rates.

As the temperature at the starting point (T_0) may not be the same for all runs, "absolute" times have little meaning. However, time intervals are meaningful. The crystallization rate (the rate of change of crystallinity with time) is given as

$$c = \frac{dx}{dt} \quad , \tag{9}$$

which is the slope in Fig. 5(a). The crystallization rate is related to the widely used rate of change of the fractional crystallization with temperature:

$$\frac{dx}{dT} = \frac{c}{q} \quad , \tag{10}$$

https://doi.org/10.1557/jmr.2011.44 Published online by Cambridge University Press

which is the slope in Fig. 5(b).

Crystallization curves show a sigmoid shape, characteristic of phase transformation processes in polymers, and are usually obtained for nonisothermal crystallization in polymers such as poly(methylene therphthalate) (PMT), PET, poly(propylene therphthalate) (PPT), and poly(butylene terephthalate) (PBT).[28]

Macroscopic crystallization in polymers starts at very low rates due to the slow, first nucleation step; crystallization rate increases during the main or bulk crystallization and then decreases as the material is depleted of crystallizable molecules. The fact that most polymers are not pure substances but mixtures of macromolecules of different masses enhances the gradual variation of crystallization rate with time. The results are the asymmetric endothermic peaks that, when integrated, give rise to the sigmoids observed.

The similarity in shape of the crystallization curves for different heating rates suggests that crystallization mechanisms are similar; variations observed during the cold crystallization may be attributed to differences in the nucleation and crystalline growth rates, but have the same morphologic crystallization mechanisms. A similar behavior was reported elsewhere for isothermal cold crystallization of PET.[14]

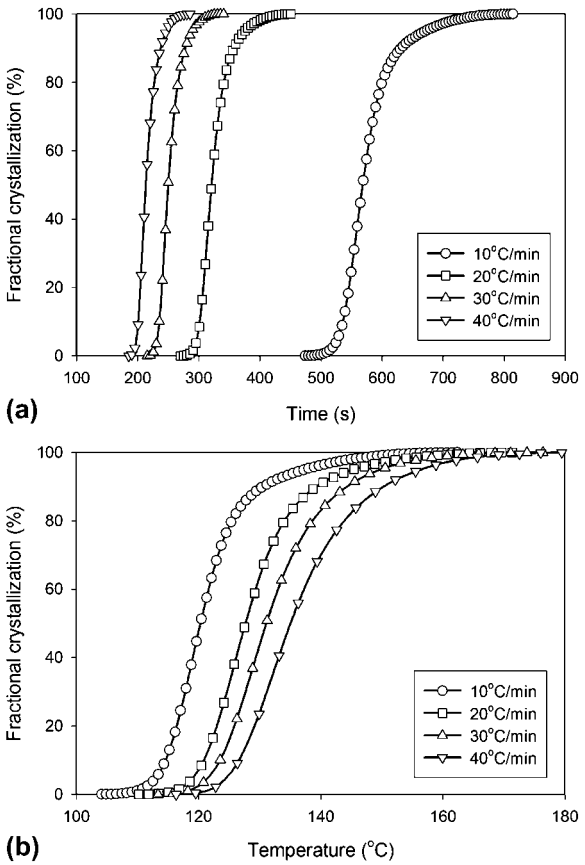


FIG. 5. Fractional crystallization of PET as a function of (a) time and (b) temperature for several values of the heating rate.

Table III shows the temperature at the midpoint ($x = 0.5$) and the temperature and time intervals for the cold crystallization, defined for the interval from 1 to 99% fractional crystallization; the 0 and 100% crystallization marks were avoided as they depend too much on the somewhat arbitrary choice of peak onset and end points.

The rate of crystallization changes continuously with time or temperature (in fact, the rate of crystallization is proportional to the DSC output). It may be convenient, from a purely phenomenological point of view, to define mean rates of crystallization for the initial, main, and final stages of the cold crystallization process:

$$\bar{c} = \frac{\Delta x}{\Delta t} \quad . \tag{11}$$

Time intervals for change in fractional crystallization were selected from 1 to 5% (initial), from 20 to 80% (main), and from 95 to 99% (final). Thus,

$$\begin{aligned} \bar{c}_{\text{initial}} &= \frac{0.05 - 0.01}{t_{0.05} - t_{0.01}} \\ \bar{c}_{\text{main}} &= \frac{0.8 - 0.2}{t_{0.8} - t_{0.2}} \\ \bar{c}_{\text{final}} &= \frac{0.99 - 0.95}{t_{0.99} - t_{0.95}} \end{aligned} \quad . \tag{12}$$

The results are shown in Table IV and represented graphically in Fig. 6. A significant increase in all crystallization

TABLE III. Temperatures for 50% of crystallization and temperature and time intervals for nonisothermal cold crystallization of PET at several heating rates.

q (°C/min)	$T_{0.5}$ (°C)	$\Delta T_c = T_{0.99} - T_{0.01}$ (°C)	$\Delta t_c = t_{0.99} - t_{0.01}$ (s)
2.5	109.9	25.6	596
5	113.8	42.1	491
7.5	114.6	38.2	297
10	120.5	39.4	230
15	123.8	35.2	138
20	127.7	41.9	124
30	130.9	42.5	85
40	134.5	46.4	70

TABLE IV. Mean crystallization rates of PET at several heating rates.

	Mean crystallization rates			
q (°C/min)	Initial (1–5%)	Main (20–80%) (0.001 s)	Final (95–99%)	Total time (1–99%) (s)
2.5	0.67	3.88	0.24	596
5	0.88	4.42	0.33	491
7.5	1.83	7.80	0.43	297
10	2.08	11.16	0.59	230
15	4.08	17.01	0.92	138
20	4.71	17.53	1.08	124
30	5.43	23.55	1.94	85
40	8.21	26.06	2.51	70

https://doi.org/10.1557/jmr.2011.44 Published online by Cambridge University Press

rates was observed with an increase in heating rate. A 16-fold rise in heating rate resulted in 12.3, 6.7, and 10.5 times amplification of the initial, main, and final crystallization rates. Total time required for full crystallization decreased 8.5 times for same rise in heating rates.

C. Crystallization kinetics

Ozawa model[20] was used to elucidate the kinetics of the cold crystallization process. Ozawa assumes that nonisothermal crystallization is governed by the same mechanism proposed by Avrami for isothermal crystallization. A most interesting feature of Ozawa model is the possibility to compare the results of crystallization during continuous cooling/heating with those obtained by means of the Avrami equation under isothermal conditions. Ozawa model requires a constant rate of temperature change, $q = dT/dt$ = constant, and has been successfully used to study nonisothermal crystallization of PET[13,11,29] and its blends[30] and copolymers.[31]

Ozawa kinetic model is given by

$$x = 1 - \exp(-K_T q^{-m}) \quad , \qquad (13)$$

where x is the fractional crystallization, q is the heating rate, and K_T and m are the Ozawa parameters, which are functions of the temperature and depend on nucleation and growth mechanisms.

From Eq. (13), we obtain

$$\ln[-\ln(1-x)] = \ln K_T + m \ln(1/q) \quad . \qquad (14)$$

Thus, Ozawa model predicts a linear relationship between $\ln[-\ln(1-x)]$ and $\ln(1/q)$ at constant temperature. Figure 7 shows such a plot taken from the integrated data (Fig. 5) and computed at four different temperatures.

Two different kinetic regimes can be clearly identified, both following Ozawa's model, but each with a different set of parameters: a primary crystallization process at low and moderate fractional crystallizations and a secondary crystallization process at higher fractional crystallizations. The critical fractional crystallization $x_{critical}$ at which the crystallization regime switches from one to other regimes increases with temperature. Table V shows the estimated Ozawa parameters for both crystallization regimes and the critical fractional crystallization.

The critical fractional crystallization that separates the two regimes turns out to be a linear function of the temperature (Fig. 8).

Ozawa's exponent m decreases with increasing crystallization temperature, following the same trend observed elsewhere for isothermal crystallization.[14] At lower temperatures, the lower growth rate favors the development of more complex morphologic structures. Ozawa's constant K_T also decreases with increasing temperatures, opposite to the trend observed for crystallization under isothermal conditions.[14] Run et al.[32] applied Ozawa model in the kinetic study of nonisothermal melt crystallization of PMT and reported an increase in both Ozawa constants (m and K_T) with an increase in the crystallization temperature. Similar trend were observed by Liu et al.[33] in a poly(aryl ether ketone). Usually, when nonisothermal crystallization from the melt is analyzed using Ozawa model, a decrease in

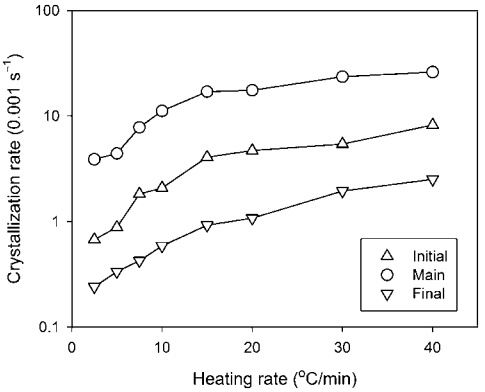


FIG. 6. Mean crystallization rates for the initial, main, and final crystallization stages for PET as functions of the heating rate.

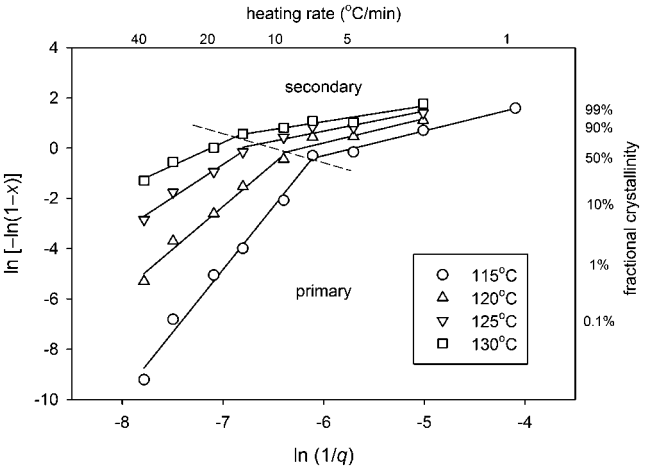


FIG. 7. Ozawa plot at several temperatures showing the different kinetics for the primary and secondary cold crystallization steps ($1/q$ in s/°C).

TABLE V. Ozawa parameters for nonisothermal cold crystallization of PET.

	Primary crystallization			Secondary crystallization	
T (°C)	ln K_T	m	$x_{critical}$ (%)	ln K_T	m
115	30.09	4.99	49	5.60	0.98
120	21.53	3.41	58	6.01	0.97
125	17.83	2.64	68	5.46	0.80
130	13.01	1.83	82	4.81	0.63

Parameters computed with heating rates are expressed in °C/s.

https://doi.org/10.1557/jmr.2011.44 Published online by Cambridge University Press

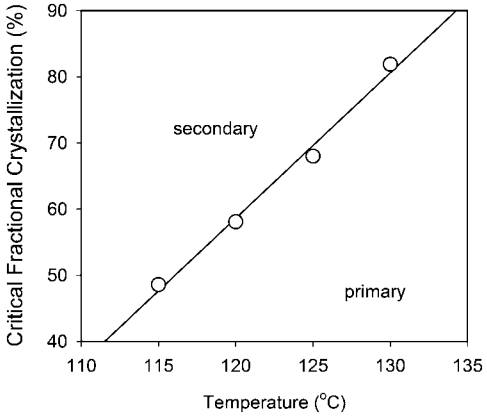


FIG. 8. Critical fractional crystallization of PET during nonisothermal cold crystallization as a function of temperature.

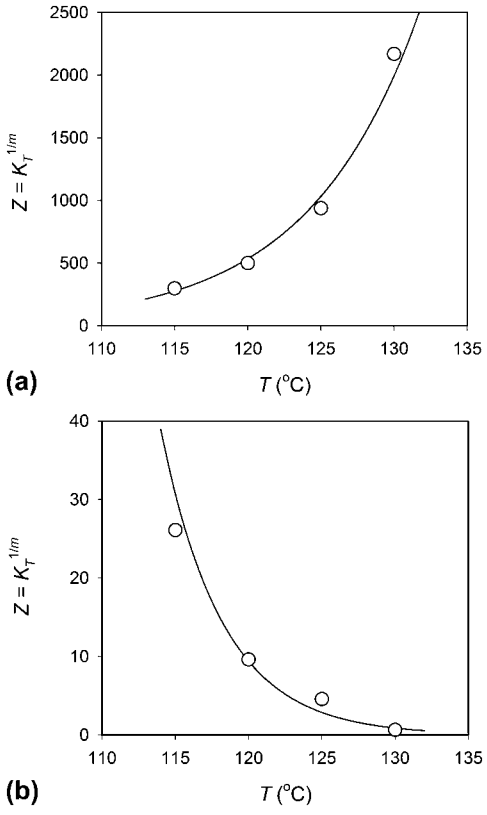


FIG. 9. *Z*-plots for the (a) primary and (b) secondary crystallization regimes of PET. Lines are best-fit exponentials.

K_T is observed, while the opposite is expected for nonisothermal cold crystallization.

According to Hieber[34] and Sajkiewicz et al.,[13] a combination of Ozawa's parameters:

$$Z = K_T^{1/m} \quad , \tag{15}$$

may be used to compare the crystallization kinetics on polymeric systems under different crystallization conditions;

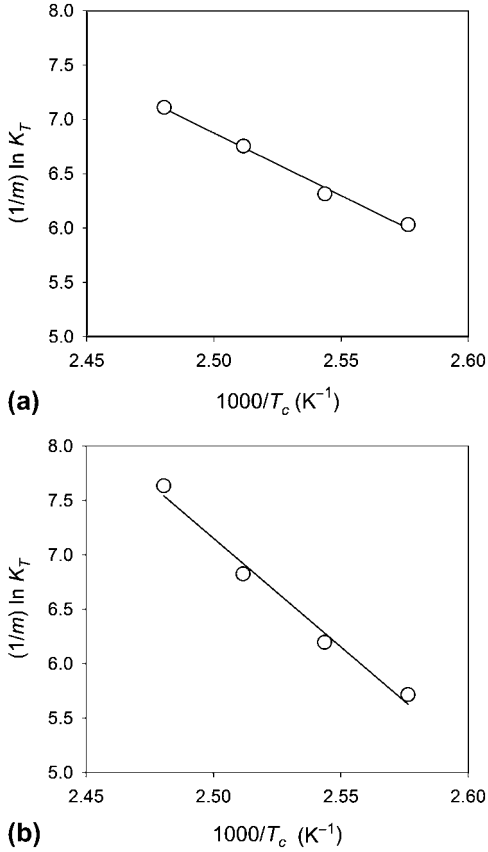


FIG. 10. Arrhenius plots for the (a) primary and (b) secondary crystallization regimes of PET.

the *Z* rate constant, with units of $(°C/min)^m$, makes possible the joint treatment of the results for isothermal and nonisothermal crystallization. Figure 9 shows the *Z* parameter as a function of crystallization temperature for both crystallization regimes observed in this work.

For the primary crystallization regime [Fig. 9(a)], *Z* increases with the crystallization temperature; a similar trend was verified for isothermal crystallization.[14] An increase in *Z* with increasing crystallization temperature was reported for PET, PPT, and PBT.[35]

For the secondary crystallization regime, a steeper increase in *Z* was observed with temperature [Fig. 9(b)]. As showed in Table V, an increase in the crystallization temperature contributes to higher $x_{critical}$ values. Thus, the secondary crystallization takes place in regions with larger impingement, which contributes to a decrease in the value of *Z* for this regime, at low crystallization temperatures ($T_c < 120$ °C). At higher crystallization temperatures, the thermal effects seem to overcome spatial limitations, leading to higher values of the *Z* parameter for the secondary crystallization than for the primary regime.[36]

Figure 9 shows that the kinetic parameter *Z* depends exponentially on the crystallization temperature for both crystallization regimes, suggesting thermally activated

https://doi.org/10.1557/jmr.2011.44 Published online by Cambridge University Press

processes, which may be approximately described by Arrhenius type expressions[22,33]:

$$Z = K_T^{1/m} = K_0 \exp\left(-\frac{\Delta E_c}{R T_c}\right) \quad , \qquad (16)$$

or

$$\left(\frac{1}{m}\right) \ln K_T = \ln K_0 - \frac{\Delta E_c}{R T_c} \quad , \qquad (17)$$

where K_0 is a temperature-independent pre-exponential factor, m is Ozawa's exponent, T_c is the cold crystallization temperature, ΔE_c is the activation energy for the crystallization process, and $R = 8.315$ J/mol·K is the ideal gas constant.

The activation energy ΔE_c can be estimated from the slope of the plots of $(1/m)\ln K_T$ versus $1/T_c$, as shown in Fig. 10. Values of 96 and 166 kJ/mol were found for the primary and secondary crystallization regimes of PET, respectively. These results are consistent with the data shown in Table V, where a decrease in Ozawa's K_T constant is observed for secondary crystallization, which may indicate that the secondary crystallization is occurring in zones with higher energy consumption.

We defer a detailed discussion of the secondary crystallization process and a possible pre-primary kinetic regime (suggested by Fig. 7, but we cannot confirm that at this point due to the resolution of the data at very low fractional crystallization) for a forthcoming paper.

IV. CONCLUSIONS

The nonisothermal cold crystallization of PET was analyzed by DSC, and the kinetic parameters were obtained using Ozawa model. Major conclusions are as follows:

(1) The glass transition and cold crystallization temperatures show a significant increase with the heating rate, whereas the melting temperature is virtually independent of the heating rate.

(2) The latent heats of crystallization and melting show a moderate decrease with the heating rate, while the difference between them is approximately constant, independent of the heating rate.

(3) The rate of crystallization rate increases substantially with an increase in the heating rate.

(4) Two different kinetic regimes were identified: a primary crystallization process at low and moderate fractional crystallizations and a secondary crystallization process at higher fractional crystallizations.

(5) Ozawa parameters (both the pre-exponential and the exponential factors) decreased with increasing crystallization temperature for both crystallization regimes.

(6) The combined kinetic parameter Z of Hieber and Sajkiewicz increased exponentially with temperature for both crystallization regimes; the activation energy was higher for the secondary crystallization regime than for the first.

ACKNOWLEDGMENTS

The authors thank Terphane (Brazil) for providing the polymer used in this work and gratefully acknowledge Conselho Nacional de Desenvolvimento Científico e Tecnológico (CNPq) and Fundação de Amparo à Ciência e Tecnologia do Estado de Pernambuco (FACEPE) (Brazil) for the financial support.

REFERENCES

1. F. Van Antwerpen and D.W. Van Krevelen: Influence of crystallization temperature, molecular weight, and additives on the crystallization kinetics of poly(ethylene terephthalate). *J. Polym. Sci., Part B: Polym. Phys. Ed.* **10**, 2423 (1972).
2. O. Verhoyen, F. Dupret, and R. Legras: Isothermal and nonisothermal crystallization kinetics of polyethylene terephthalate: Mathematical modeling and experimental measurement. *Polym. Eng. Sci.* **38**, 1594 (1998).
3. D.S. Achilias, G.Z. Papageorgiou, and G.P. Karayannidis: Isothermal and nonisothermal crystallization kinetics of poly(propylene terephthalate). *J. Polym. Sci., Part B: Polym. Phys.* **42**, 3775 (2004).
4. G.C. Alfonso: Crystallization in polymer blends. In *Integration of Fundamental Polymer Science and Technology,* Vol. 5, edited by P. J. Lemstra and L.A. Keintjen (Elsevier, Amsterdam and London, 1991), p. 143.
5. L. Mandelkern: *Crystallization of Polymers* (McGraw-Hill, New York, 1964).
6. T.Y. Chen, V.W. Wang, and M.J. Bozarth: Crystallization and its effect on the processing of polypropylene. *J. Reinforc. Plast. Compos.* **12**, 686 (1993).
7. Y.P. Khanna, A.C. Reimschuessel, A. Banerjie, and C. Altman: Memory effects in polymers. II. Processing history vs crystallization rate of nylon 6—Observation of phenomenon and product behavior. *Polym. Eng. Sci.* **28**, 1600 (1988).
8. A. Elmoumni, H.H. Winter, A.J. Waddon, and H. Fruitwala: Correlation of material and processing time scales with structure development in isotactic polypropylene crystallization. *Macromolecules* **36**, 6453 (2003).
9. M.L. Addonizio, E. Martuscelli, and C. Silvestre: Study of the nonisothermal crystallization of poly(ethylene oxide)/poly(methyl methacrylate) blends. *Polymer (Guildf.)* **28**, 183 (1987).
10. S.A. Jabarin: Crystallization kinetics of polyethylene terephthalate. II. Dynamic crystallization of PET. *J. Appl. Polym. Sci.* **34**, 97 (1987).
11. D.M. Fann, S.K. Huang, and J.Y. Lee: Kinetics and thermal crystallinity of recycled PET. I. Dynamic cooling crystallization studies on blends recycled with engineering PET. *J. Appl. Polym. Sci.* **61**, 1375 (1996).
12. X. Lu and J.N. Hay: The effect of phisycal aging on the rates of cold crystallization of poly(ethylene terephthalate). *Polymer (Guildf.)* **41**, 7427 (2000).
13. P. Sajkiewicz, L. Carpaneto, and A. Wasiak: Application of the Ozawa model to non-isothermal crystallization of poly (ethylene terephthalate). *Polymer (Guildf.)* **42**, 5365 (2001).
14. R.M.R. Wellen and M.S. Rabello: The kinetics of isothermal crystallization and tensile properties of poly(ethylene) terephthalate. *J. Mater. Sci.* **40**, 6099 (2005).

https://doi.org/10.1557/jmr.2011.44 Published online by Cambridge University Press

15. B. Wunderlich: *Thermal Analysis of Polymeric Materials* (Springer, Berlin, 2005).
16. J.B. Menard: Thermal transitions and their measurement, in *Performance of Plastics*, edited by W. Brostow (Hanser, Munich, 2000).
17. P.D. Hong, W.T. Chung, and C.F. Hsu: Crystallization kinetics and morphology of poly(trimethylene terephthalate). *Polymer (Guildf.)* **43**, 3335 (2002).
18. R.M.R. Wellen and M.S. Rabello: Non-isothermal cold crystallization kinetics and morphology of PET + SAN blends. *J. Appl. Polym. Sci.* **116**, 1077 (2010).
19. H.E. Kissinger: Variation of the peak temperature with heating rate in differential thermal analysis. *J. Res. Natl. Bur. Stand.* **57**, 217 (1956).
20. P. Cebe and S. Hong: Crystallization behaviour of poly(ether-ether-ketone). *Polymer (Guildf.)* **27**, 1183 (1986).
21. N. Apiwanthanakorn, P. Supaphol, and M. Nithitanakul: Non-isothermal melt-crystallization kinetics of poly(trimethylene terephthalate). *Polym. Test.* **23**, 817 (2004).
22. P. Cebe: Non-isothermal crystallization of poly(ether ether ketone)—Aromatic polymer composite. *Polym. Comp.* **9**, 271 (1988).
23. N. Yoshihara, M. Shibaya, and H. Ishihara: Cold crystallization behaviors of poly(ethylene terephthalate). *J. Polym. Eng.* **25**, 97 (2005).
24. L.W. Jang, K.H. Lee, D.C. Lee, J.S. Yoon, I. Chin, and H.J. Choi: Alternating copolymers as compatibilizer for blends of poly (ethylene terephthalate) and polystyrene. *J. Appl. Polym. Sci.* **78**, 1998 (2000).
25. A. Metha, U. Gaur, and B. Wunderlich: Equilibrium melting parameters of poly(ethylene terephthalate). *J. Polym. Sci., Part B: Polym. Phys. Ed.* **16**, 289 (1978).
26. Y. Kong and J.N. Hay: The measurement of the crystallinity of polymers by DSC. *Polymer (Guildf.)* **43**, 3873 (2002).
27. D.W. van Krevelen: *Properties of Polymers* (Elsevier, Amsterdam, 1990).
28. N. Dangseeyun, P. Supaphol, and M. Nithitanakul: Thermal, crystallization, and rheological characteristics of poly(trimethylene terephthalate)/poly(butylene terephthalate) blends. *Polym. Test.* **23**, 187 (2004).
29. T. Ozawa: Kinetics of non-isothermal crystallization. *Polymer (Guildf.)* **12**, 150 (1971).
30. C.F. Ou and C.C. Lin: Blends of polyethylene terephthalate with co [poly(ethylene terephthalate-p-oxybenzoate)] I. Crystallization kinetics by DSC study. *J. Appl. Polym. Sci.* **54**, 1223 (1994).
31. Y. Zhang and L. Gu: Study of non-isothermal crystallization kinetics and sequence distribuition in poly (ethylene terephthalate-co-isophthalate). *Eur. Polym. J.* **36**, 759 (2000).
32. M. Run, C. Yao, and Y. Wang: Morphology, isothermal and non-isothermal crystallization kinetics of poly(methylene terephthalate). *Eur. Polym. J.* **42**, 655 (2006).
33. T. Liu, Z. Mo, and H. Zhang: Nonisothermal crystallization behavior of a novel poly (aryl ether ketone): PEDEKmK. *J. Appl. Polym. Sci.* **67**, 815 (1998).
34. C.A. Hieber: Correlations for the quiescent crystallization kinetics of isotactic polypropylene and poly(ethylene terephthalate). *Polymer (Guildf.)* **36**, 1455 (1995).
35. P. Supaphol, N. Dangseeyun, P. Srimoaon, and M. Nithitanakul: Nonisothermal melt-crystallization kinetics for three linear aromatic polyesters. *Thermochim. Acta* **406**, 207 (2003).
36. J. Yang, P. Pan, T. Dong, and Y. Inoue: Crystallization kinetics and crystalline structure of biodegradable poly(ethylene adipate). *Polymer (Guildf.)* **51**, 807 (2010).

https://doi.org/10.1557/jmr.2011.44 Published online by Cambridge University Press